



12-2018

The Basins of Convergence in the Planar Restricted Four-body Problem with Variable Mass

Amit Mittal

ARSD College, University of Delhi

Monika Arora

Miranda House, University of Delhi

Md S. Suraj

Sri Aurobindo College, University of Delhi

Rajiv Aggarwal

Deshbandhu College, University of Delhi

Follow this and additional works at: <https://digitalcommons.pvamu.edu/aam>



Part of the [Dynamic Systems Commons](#), and the [Other Physics Commons](#)

Recommended Citation

Mittal, Amit; Arora, Monika; Suraj, Md S.; and Aggarwal, Rajiv (2018). The Basins of Convergence in the Planar Restricted Four-body Problem with Variable Mass, *Applications and Applied Mathematics: An International Journal (AAM)*, Vol. 13, Iss. 2, Article 39.

Available at: <https://digitalcommons.pvamu.edu/aam/vol13/iss2/39>

This Article is brought to you for free and open access by Digital Commons @PVAMU. It has been accepted for inclusion in *Applications and Applied Mathematics: An International Journal (AAM)* by an authorized editor of Digital Commons @PVAMU. For more information, please contact hvkoshy@pvamu.edu.



The Basins of Convergence in the Planar Restricted Four-body Problem with Variable Mass

¹Amit Mittal, ²Monika Arora, ³Md Sanam Suraj and ⁴Rajiv Aggarwal

¹Department of Mathematics
ARSD College, University of Delhi
New Delhi, India
to.amitmittal@gmail.com

²Department of Mathematics
Miranda House, University of Delhi
New Delhi, India
monikaarora1@gmail.com

³Department of Mathematics
Sri Aurobindo College, University of Delhi
New Delhi, India
mdsanamsuraj@gmail.com

⁴Department of Mathematics
Deshbandhu College, University of Delhi
New Delhi, India
rajiv_agg1973@yahoo.com

Received: November 17, 2017; Accepted: March 22, 2018

Abstract

We have studied the existence, location and stability of the libration points in the model of restricted four-body problem (R4BP) with variable mass. It is assumed that three primaries, one dominant primary and the other two with equal masses, are always forming an equilateral triangle. We have determined the equations of motion of the above mentioned problem for the fourth body which is

an infinitesimal mass. The libration points have been determined numerically for different values of the parameters considered. It is found that there are eight or ten libration points out of which six are non-collinear and two or four are collinear depending upon the values of mass parameter and the constant of proportionality occurring in Jeans' law. The regions of motion of the infinitesimal mass have been drawn and investigated. We have also examined the stability of each libration point and found that all the libration points are unstable. Further, the Newton-Raphson basins of attraction are drawn for different set of parameters used.

Keywords: R4BP; Libration Point; Zero Velocity Curve; Newton-Raphson Basins of Attraction

MSC 2010 No.: 37N05, 70F07, 70F15

1. Introduction

The few-body problem (specially three and four-body problem) has always captivated many mathematicians and astronomers. History of the restricted three-body problem begins with Newton (1687), where he considered the motion of the Earth and Moon around the Sun. Further, a special form of the general three-body problem was suggested by Euler (1767) and he was the first to formulate the circular restricted three-body problem in a rotating coordinate system.

Later on, several modifications have been proposed for the study of the motion of the test particle in the restricted three-body problem to be more realistic. A large number of researchers and scientists devoted their sweat to examine the existence and stability of the libration points in the restricted three-body problem: by including the small perturbations in the Coriolis and centrifugal forces (for example, Bhatnagar and Hallan (1978), the photogravitational effect (for example, Kumar and Choudhry (1986), Bhatnagar and Chawla (1979), Abouelmagd (2012)), the additions of the oblateness coefficient to the potential (for example, Sharma and Subba Rao (1975, 1976)). The existence of periodic orbits on the same problem has been discussed by many authors: (for example, Sharma (1981), Mittal et al. (2009a,b)). Suraj et al. (2014) have studied the photo-gravitational version of the R3BP by taking the primaries as heterogeneous spheroid with three layers.

It was Shrivastava and Ishwar (1983), who introduced variable mass of the test particle in the restricted problem of three bodies. Further, Singh and Ishwar (1984) have studied the effect of perturbations on the location of equilibrium points with variable mass in the restricted problem of three bodies while Singh and Ishwar (1985) have extended their study to examine the stability of the equilibrium points. Later, Singh (2003) has examined the photogravitational version of the restricted three-body problem by taking more massive primary as variable while Singh and Leke (2010) have taken both the primaries as luminous body as well as their masses as variable.

In the same vein, many authors and scientists have extended these ideas in the restricted four-body problem. The existence of equilibrium points and their stability (for example, Baltagiannis and Papadakis (2011), Asique et al. (2015b)), with radiation effect (for example, Papadouris and

Papadakis (2013), Suraj and Hassan (2014), Asique et al. (2015a), Singh and Vincent (2015b, 2016)), including oblateness of the primaries (for example, Kumari and Kushvah (2014)), including triaxiality of the primaries (for example, Asique et al. (2016), Asique et al. (2017), Suraj et al. (2017)), and effect of the Coriolis and centrifugal forces (for example, Singh and Vincent (2015a), Suraj et al. (2017)).

In a series of papers, Kaur and Aggarwal (2012, 2013, 2014) and Aggarwal and Kaur (2014) have extended Robe's restricted three body problem to Robe's 2+2 body problem. By taking the primaries as oblate Roche ellipsoid, they have discussed the existence and stability of the libration points in all the cases.

Recently, Mittal et al. (2016) have shown the existence and locations of the libration points in the circular restricted four-body problem with variable mass and found that there exist eight libration points which are substantially influenced by the parameters used. Moreover, they have investigated the stability of the libration points for $\alpha > 0$ in the linear sense and found that all the libration points are unstable for all combination of mass parameter and constant of proportionality α . In addition, they have also discussed the regions of possible motion and revealed that these regions are highly influenced by the values of Jacobian constant as well as by the perturbation parameters.

The present paper is continuation of Mittal et al. (2016). It is the first time, we have numerically investigated the influence of the mass parameter μ and parameter α on the geometry and the shape of the Newton-Raphson basins of convergence in a systematic way. These facts lead to the novel contribution of our work.

The present paper has following structure: the important properties of the dynamical system are presented in Sect. 2. The parametric evolution of the libration points is presented in Sect. 3. In the Sect. 4, we have discussed how the mass parameter and perturbation parameter influence the possible regions of motion. The following section deals with the stability of the obtained libration points. The numerical results corresponding to the evolution of the Newton-Raphson basins of convergence associated with the libration points are presented in Sec. 6. The paper ends with Sec.7, where we have described the obtained results in detail.

2. Description of the mathematical model

This section deals with the formulation of the restricted four-body problem with variable mass. A dimensionless barycentric rotating system of co-ordinate $Oxyz$ is taken into consideration, where three primary bodies of masses m_1, m_2 and m_3 ($m_1 \geq m_2 = m_3$) situated at the vertices of an equilateral triangle having side l moving in their circular orbits with angular velocity ω about the center of mass O . The center of mass O is taken as the origin of the co-ordinate system, the line passing through the primary m_1 and O is taken as x -axis, the line passing through O and perpendicular to x -axis and in the plane of motion of the primaries is taken as y -axis. The line passing through origin and perpendicular to xy -plane is taken as z -axis (see Figure 1).

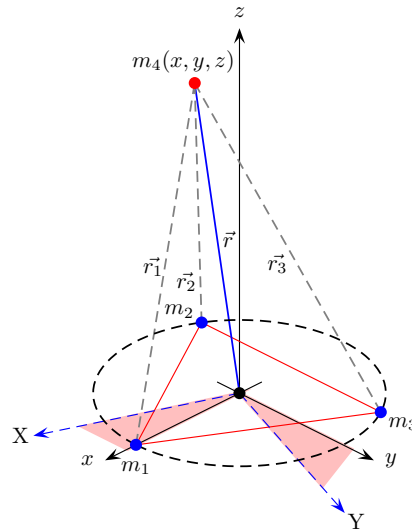


Figure 1. The configuration of the restricted four-body problem with variable mass

Then, the co-ordinates of the primaries are given by the following relations (Baltagiannis and Papadakis (2011))

$$\begin{aligned}x_1 &= \frac{|K|M}{K}, \quad y_1 = 0, \\x_2 &= -\frac{|K|[(m_2 - m_3)m_3 + m_1(2m_2 + m_3)]}{2KM}, \\y_2 &= \frac{\sqrt{3}}{2} \frac{m_3}{m_2^{3/2}} \frac{\sqrt{m_2^3}}{M}, \\x_3 &= -\frac{|K|}{2\sqrt{M}}, \\y_3 &= -\frac{\sqrt{3}}{2} \frac{1}{m_2^{1/2}} \frac{\sqrt{m_2^3}}{M}, \\z_1 &= z_2 = z_3 = 0,\end{aligned}$$

where

$$\begin{aligned}|K| &= m_2(m_3 - m_2) + m_1(m_2 + 2m_3), \\M &= \sqrt{m_2^2 + m_2m_3 + m_3^2}.\end{aligned}$$

Let the co-ordinates of the infinitesimal mass $m_4 = m$ be (x, y, z) . Adopting the terminology of Mittal et al. (2016), the coordinates of the primaries are: $P_1(x_1, y_1, z_1) = (m_2\sqrt{3}, 0, 0)$, $P_2(x_2, y_2, z_2) = (-\frac{\sqrt{3}}{2}(1 - 2m_2), -\frac{1}{2}, 0)$ and $P_3(x_3, y_3, z_3) = (-\frac{\sqrt{3}}{2}(1 - 2m_2), \frac{1}{2}, 0)$.

The kinetic energy T in the rotating frame of reference $Oxyz$ is:

$$\begin{aligned}T &= \frac{1}{2}m[(\dot{x} - \omega y)^2 + (\dot{y} + \omega x)^2 + \dot{z}^2], \\&= T_0 + T_1 + T_2,\end{aligned}\tag{1}$$

where

$$T_0 = \frac{1}{2}m(\dot{x}^2 + \dot{y}^2 + \dot{z}^2),$$

$$T_1 = m\omega(xy - \dot{x}y),$$

$$T_2 = \frac{1}{2}m\omega(x^2 + y^2).$$

The potential energy V is:

$$V = -Gm \left\{ \frac{m_1}{r_1} + m_2 \left(\frac{1}{r_2} + \frac{1}{r_3} \right) \right\}, \quad (2)$$

where G is gravitational constant and

$$r_1^2 = (x - x_1)^2 + y^2 + z^2,$$

$$r_2^2 = (x - x_2)^2 + (y - y_2)^2 + z^2,$$

$$r_3^2 = (x - x_3)^2 + (y - y_3)^2 + z^2.$$

Let the modified potential energy be $U = V - T_2$.

Therefore, the lagrangian becomes:

$$L = \frac{1}{2}m(\dot{x}^2 + \dot{y}^2 + \dot{z}^2) + m\omega(xy - \dot{x}y) - U. \quad (3)$$

The equations of motion of the fourth particle is:

$$\begin{aligned} \frac{d}{dt} \left(\frac{\partial L}{\partial \dot{x}} \right) - \frac{\partial L}{\partial x} &= 0, \\ \frac{d}{dt} \left(\frac{\partial L}{\partial \dot{y}} \right) - \frac{\partial L}{\partial y} &= 0, \\ \frac{d}{dt} \left(\frac{\partial L}{\partial \dot{z}} \right) - \frac{\partial L}{\partial z} &= 0. \end{aligned} \quad (4)$$

Now, we choose $\frac{m_2}{m_1+m_2+m_3} = \mu$ and units of mass, length and time are so chosen that $m_1 + m_2 + m_3 = 1$, $l = 1$ and $G = 1$ respectively. Therefore, angular velocity $\omega = 1$, masses $m_2 = m_3 = \mu$ and $m_1 = 1 - 2\mu$. Thus, the coordinates of the primaries P_1 , P_2 and P_3 become: $P_1(x_1, y_1, z_1) = (\sqrt{3}\mu, 0, 0)$, $P_2(x_2, y_2, z_2) = (-\frac{\sqrt{3}}{2}(1 - 2\mu), -\frac{1}{2}, 0)$, and $P_3(x_3, y_3, z_3) = (-\frac{\sqrt{3}}{2}(1 - 2\mu), \frac{1}{2}, 0)$.

Hence, the equations of motion of the restricted problem of four bodies, when mass of the infinitesimal body varies with respect to time t , are:

$$\begin{aligned} \ddot{x} - 2\omega\dot{y} + \frac{\dot{m}}{m}(\dot{x} - \omega y) &= -\frac{1}{m} \frac{\partial U}{\partial x}, \\ \ddot{y} + 2\omega\dot{x} + \frac{\dot{m}}{m}(\dot{y} + \omega x) &= -\frac{1}{m} \frac{\partial U}{\partial y}, \\ \ddot{z} + \frac{\dot{m}}{m}\dot{z} &= -\frac{1}{m} \frac{\partial U}{\partial z}, \end{aligned} \quad (5)$$

where

$$U = \frac{m}{2}(x^2 + y^2) + m \left\{ \frac{1 - 2\mu}{r_1} + \mu \left(\frac{1}{r_2} + \frac{1}{r_3} \right) \right\}. \quad (6)$$

According to Jeans' Law (1928)

$$\frac{dm}{dt} = -\alpha m^n, \quad (7)$$

where α is constant of proportionality, the exponent $n \in [0.4, 4.4]$ for the star of the main sequence. Now, we introduce the space-time transformations (Meshcherskii (1949), Meshcherskii (1952)) which preserve the dimensions of the space and time

$$\begin{aligned} \xi &= \gamma^q x, & \eta &= \gamma^q y, & \zeta &= \gamma^q z, \\ d\tau &= \gamma^v dt, & r_i &= \gamma^{-q} \rho_i, \quad (i = 1, 2, 3), \end{aligned}$$

such that $\gamma = \frac{m}{m_{ini}}$, m_{ini} is the mass of the fourth body at the initial time ($t = 0$). Shrivastava and Ishwar (1983) have stated that the applicable values of (n, q, v) are $n = 1$, $q = \frac{1}{2}$, and $v = 0$. Hence, the velocity and acceleration components are read as:

$$\begin{aligned} \gamma^{\frac{1}{2}} \dot{x} &= \xi' + \frac{1}{2} \alpha \xi, \\ \gamma^{\frac{1}{2}} \dot{y} &= \eta' + \frac{1}{2} \alpha \eta, \\ \gamma^{\frac{1}{2}} \dot{z} &= \zeta' + \frac{1}{2} \alpha \zeta, \\ \gamma^{\frac{1}{2}} \ddot{x} &= \xi'' + \alpha \xi' + \frac{1}{4} \alpha^2 \xi, \\ \gamma^{\frac{1}{2}} \ddot{y} &= \eta'' + \alpha \eta' + \frac{1}{4} \alpha^2 \eta, \\ \gamma^{\frac{1}{2}} \ddot{z} &= \zeta'' + \alpha \zeta' + \frac{1}{4} \alpha^2 \zeta, \end{aligned} \quad (8)$$

where

$$(') = \frac{d}{d\tau}, (\cdot) = \frac{d}{dt}, \& \frac{d}{dt} = \frac{d}{d\tau}.$$

Using the procedure of Mittal et al. (2016) and Equations (5-8), the equations of motion in the transformed co-ordinates are:

$$\begin{aligned} \ddot{\xi} - 2\dot{\eta} &= W_\xi, \\ \ddot{\eta} + 2\dot{\xi} &= W_\eta, \\ \ddot{\zeta} &= W_\zeta, \end{aligned} \quad (9)$$

where

$$\begin{aligned} W &= \frac{1}{2} \left(1 + \frac{\alpha^2}{4} \right) (\xi^2 + \eta^2) + \gamma^{3/2} \left(\frac{1-2\mu}{\rho_1} + \frac{\mu}{\rho_2} + \frac{\mu}{\rho_3} \right) + \frac{\alpha^2}{8} \zeta^2, \\ \rho_1^2 &= \left(\xi - \sqrt{3}\mu\gamma^{1/2} \right)^2 + \eta^2 + \zeta^2, \\ \rho_2^2 &= \left(\xi + \frac{\sqrt{3}}{2}(1-2\mu)\gamma^{1/2} \right)^2 + \left(\eta + \frac{1}{2}\gamma^{1/2} \right)^2 + \zeta^2, \\ \rho_3^2 &= \left(\xi + \frac{\sqrt{3}}{2}(1-2\mu)\gamma^{1/2} \right)^2 + \left(\eta - \frac{1}{2}\gamma^{1/2} \right)^2 + \zeta^2. \end{aligned} \quad (10)$$

The equations of motion (9) possess only one integral of motion known as Jacobi integral which is given by the equation:

$$J(\xi, \eta, \zeta, \dot{\xi}, \dot{\eta}, \dot{\zeta}) = (\dot{\xi}^2 + \dot{\eta}^2 + \dot{\zeta}^2) - 2W + C + 2 \int_0^t W_t dt = 0, \quad (11)$$

where C is similar to Jacobi constant.

3. Libration points

Lagrange showed that a classical restricted three-body problem possesses five stationary solutions which are also known as libration points or Lagrangian points. Baltagiannis and Papadakis (2011) found that there exist at most ten libration points in the classical restricted four-body problem. The libration points are obtained by solving the equations:

$$\begin{aligned} W_\xi &= 0, \\ W_\eta &= 0, \\ W_\zeta &= 0, \end{aligned} \quad (12)$$

where

$$\begin{aligned} W_\xi &= \left(1 + \frac{\alpha^2}{4}\right)\xi - \gamma^{3/2} \left\{ \frac{(1-2\mu)(\xi - \sqrt{3}\mu\gamma^{1/2})}{\rho_1^3} + \mu \left(\frac{\xi + \frac{\sqrt{3}}{2}(1-2\mu)\gamma^{1/2}}{\rho_2^3} \right) + \mu \left(\frac{\xi + \frac{\sqrt{3}}{2}(1-2\mu)\gamma^{1/2}}{\rho_3^3} \right) \right\}, \\ W_\eta &= \left(1 + \frac{\alpha^2}{4}\right)\eta - \gamma^{3/2} \left\{ \frac{(1-2\mu)\eta}{\rho_1^3} + \mu \left(\frac{\eta + \frac{1}{2}\gamma^{1/2}}{\rho_2^3} \right) + \mu \left(\frac{\eta - \frac{1}{2}\gamma^{1/2}}{\rho_3^3} \right) \right\}, \\ W_\zeta &= \frac{\alpha^2}{4}\zeta - \gamma^{3/2} \left\{ \frac{(1-2\mu)\zeta}{\rho_1^3} + \frac{\mu\zeta}{\rho_2^3} + \frac{\mu\zeta}{\rho_3^3} \right\}. \end{aligned}$$

The intersections of Equations (12) define the locations of the libration points in this problem. The location of these libration points for fixed value of $\gamma = 0.4$ and varying values of μ and α are shown in Figure 2. We strongly believe that the number and location of these libration points depend on the mass parameter μ and constant α . We have further observed that there exist eight libration points out of which two are collinear and rest are non-collinear (see panels (a) and (b) of Figure 2) whereas, panel (c) shows there exist ten libration points (four collinear and six non-collinear). The libration points $L_{1,2,9,10}$ denote the collinear libration points which lie on the ξ -axis and $L_{3,4,5,6,7,8}$ are non-collinear libration points. It may be noted that for fixed value of $\mu = 0.3$, we may find a critical value of α viz. α_c . When $\alpha < \alpha_c$, there exist ten libration points and for $\alpha > \alpha_c$, there exist eight libration points.

The positions of the libration points are determined numerically for different values of the parameters $0 < \mu \leq \frac{1}{3}$, $0 \leq \alpha \leq 2.2$ and $\gamma = 0.4$ which are shown in the tables (1, 2, 3). We find that numerical and graphical results are in excellent agreement.

Table 1. Libration points of the R4BP with variable mass in $\xi\eta$ -plane for $\mu = 0.019$

α	L_1	L_2	$L_{3,4}$	$L_{5,6}$	$L_{7,8}$
0.5	(0.627795, 0)	(-0.605112, 0)	(-0.429138, ± 0.25915)	(-0.125826, ± 0.599354)	(-0.628948, ± 0.376772)
0.6	(0.622571, 0)	(-0.59931, 0)	(-0.428035, ± 0.258571)	(-0.127665, ± 0.593476)	(-0.626815, ± 0.375542)
0.7	(0.61662, 0)	(-0.592712, 0)	(-0.426714, ± 0.257882)	(-0.12979, ± 0.58675)	(-0.624436, ± 0.374167)
0.8	(0.610033, 0)	(-0.585426, 0)	(-0.425164, ± 0.257079)	(-0.132181, ± 0.579267)	(-0.621868, ± 0.372678)
1.25	(0.574962, 0)	(-0.547063, 0)	(-0.415107, ± 0.252061)	(-0.145697, ± 0.538612)	(-0.609926, ± 0.365327)
1.34	(0.567314, 0)	(-0.538816, 0)	(-0.412441, ± 0.250792)	(-0.148845, ± 0.529531)	(-0.606736, ± 0.363846)
1.5	(0.553523, 0)	(-0.524066, 0)	(-0.407132, ± 0.248355)	(-0.154739, ± 0.512916)	(-0.602372, ± 0.361281)
2.2	(0.494474, 0)	(-0.462709, 0)	(-0.375411, ± 0.237126)	(-0.184373, ± 0.436608)	(-0.586111, ± 0.351661)

Table 2. Libration points of the R4BP with variable mass in $\xi\eta$ -plane for $\mu = 0.3$

α	L_1	L_2	$L_{3,4}$	$L_{5,6}$	$L_{7,8}$	L_9	L_{10}
0.5	(0.729199, 0)	(-0.580932, 0)	(0.238986, ± 0.520725)	(0.027247, ± 0.148229)	(-0.423144, ± 0.606447)	(-0.084413, 0)	(-0.170613, 0)
0.6	(0.724793, 0)	(-0.574036, 0)	(0.235994, ± 0.514866)	(0.027948, ± 0.149171)	(-0.420706, ± 0.603077)	(-0.083238, 0)	(-0.173473, 0)
0.7	(0.719785, 0)	(-0.566082, 0)	(0.23255, ± 0.508136)	(0.0287844, ± 0.1503)	(-0.41794, ± 0.59925)	(-0.0819309, 0)	(-0.176802, 0)
0.8	(0.714255, 0)	(-0.557143, 0)	(0.228691, ± 0.500614)	(0.029758, ± 0.151625)	(-0.414891, ± 0.595028)	(-0.0805175, 0)	(-0.180593, 0)
1.25	(0.685068, 0)	(-0.506426, 0)	(0.207131, ± 0.458964)	(0.036011, ± 0.16034)	(-0.398902, ± 0.572806)	(-0.073423, 0)	(-0.203592, 0)
1.34	(0.678762, 0)	(-0.494404, 0)	(0.202145, ± 0.449425)	(0.0376742, ± 0.162716)	(-0.39547, ± 0.56802)	(-0.0719443, 0)	(-0.209535, 0)
1.5	(0.667447, 0)	(-0.471392, 0)	(0.192814, ± 0.431667)	(0.0410349, ± 0.167584)	(-0.389333, ± 0.559446)	(-0.0693172, 0)	(-0.22158, 0)
2.2	(0.619584, 0)	-	(0.142845, ± 0.338821)	(0.0658814, ± 0.20585)	(-0.363815, ± 0.523605)	(-0.0583929, 0)	-

Table 3. Libration points of the R4BP with variable mass in $\xi\eta$ -plane for $\alpha = 1.5$

μ	L_1	L_2	$L_{3,4}$	$L_{5,6}$	$L_{7,8}$	L_9	L_{10}
0.005	(0.547269, 0)	(-0.539519, 0)	(-0.447289, ± 0.262238)	(-0.171278, ± 0.514788)	(-0.584954, ± 0.341107)	-	-
0.01	(0.549503, 0)	(-0.534002, 0)	(-0.4308, ± 0.25608)	(-0.165377, ± 0.514131)	(-0.594337, ± 0.350056)	-	-
0.019	(0.553523, 0)	(-0.524066, 0)	(-0.407132, ± 0.248355)	(-0.154739, ± 0.512916)	(-0.602372, ± 0.361281)	-	-
0.04	(0.562885, 0)	(-0.500852, 0)	(-0.362797, ± 0.23638)	(-0.129832, ± 0.509907)	(-0.606452, ± 0.379871)	-	-
0.08	(0.580601, 0)	(-0.456448, 0)	(-0.292336, ± 0.221274)	(-0.0820345, ± 0.503411)	(-0.59503, ± 0.407139)	-	-
0.1	(0.589369, 0)	(-0.434089, 0)	(-0.259939, ± 0.215266)	(-0.0579396, ± 0.499721)	(-0.584852, ± 0.419647)	-	-
0.2	(0.631464, 0)	(-0.307001, 0)	(-0.107852, ± 0.190527)	(0.0649507, ± 0.474955)	(-0.507966, ± 0.48419)	-	-
0.3	(0.667447, 0)	(-0.471392, 0)	(0.192814, ± 0.431667)	(0.0410349, ± 0.167584)	(-0.389333, ± 0.559446)	(-0.0693172, 0)	(-0.22158, 0)

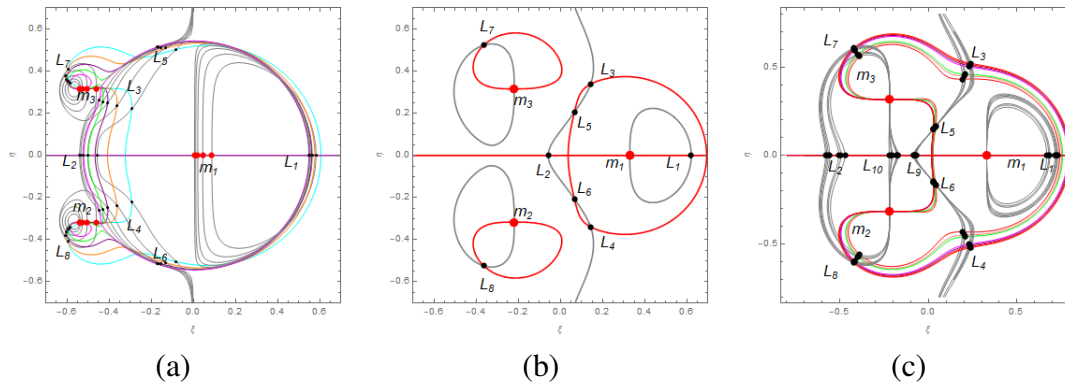


Figure 2. The locations of libration points in the restricted four-body problem with variable mass for fixed $\gamma = 0.4$. (a) $\alpha = 1.5$ and varying $\mu = 0.005, 0.01, 0.019, 0.04, 0.08$ (b) $\mu = 0.3$ and $\alpha = 2.2$. (c) $\mu = 0.3$ and varying $\alpha = 0.5, 0.6, 0.7, 0.8, 1.25, 1.34, 1.5$. The **red dots** show the position of the primaries and **black dots** show the location of the libration points

4. Regions of motion

The zero velocity curves of our problem are determined by using the relation $2W - C - 2 \int_0^t W_t dt = 0$. The motion of the test particle is possible when $2W - C - 2 \int_0^t W_t dt \geq 0$. In Figure 3, ZVCs have been drawn for fixed energy constant $C = C_{L_{5,6}} = 1.4245$, $\gamma = 0.4$, $\mu = 0.3$ and varying α , ($0 \leq \alpha \leq 2.2$). In panel (a), $\alpha = 0.5$, it is observed that the fourth particle can move in the white circular regions near the primaries and is restricted to cross the boundaries of the shaded region. Two limiting situations are observed at L_5 and L_6 . In panel (b), $\alpha = 0.8$, corridors are available at

$L_{5,6,7,8}$ and a limiting situation is observed at L_1 . The entire forbidden region is divided into three disjoint regions containing $L_{2,9,10}$, L_3 and L_4 respectively. Now, the fourth particle is free to move from one primary to another but restricted to move in the shaded regions. In panel (c), $\alpha = 1.25$, the region of motion increases and allow the test particle to move anywhere in the white region. Here, the three disjoint regions shrink towards $L_{2,9,10}$, L_3 and L_4 respectively. In panel (d), it is observed for $\alpha = 2.2$, the forbidden regions containing the libration points L_3 and L_4 disappear completely at these libration points and the forbidden region containing the libration points L_2 , L_9 and L_{10} shrinks to a triangular island which contains L_9 . Now, the fourth particle is allowed to move freely in the white region and restricted to move in the shaded region. Further increase in α , the forbidden region disappears completely at L_9 and the test particle is free to move in the space.

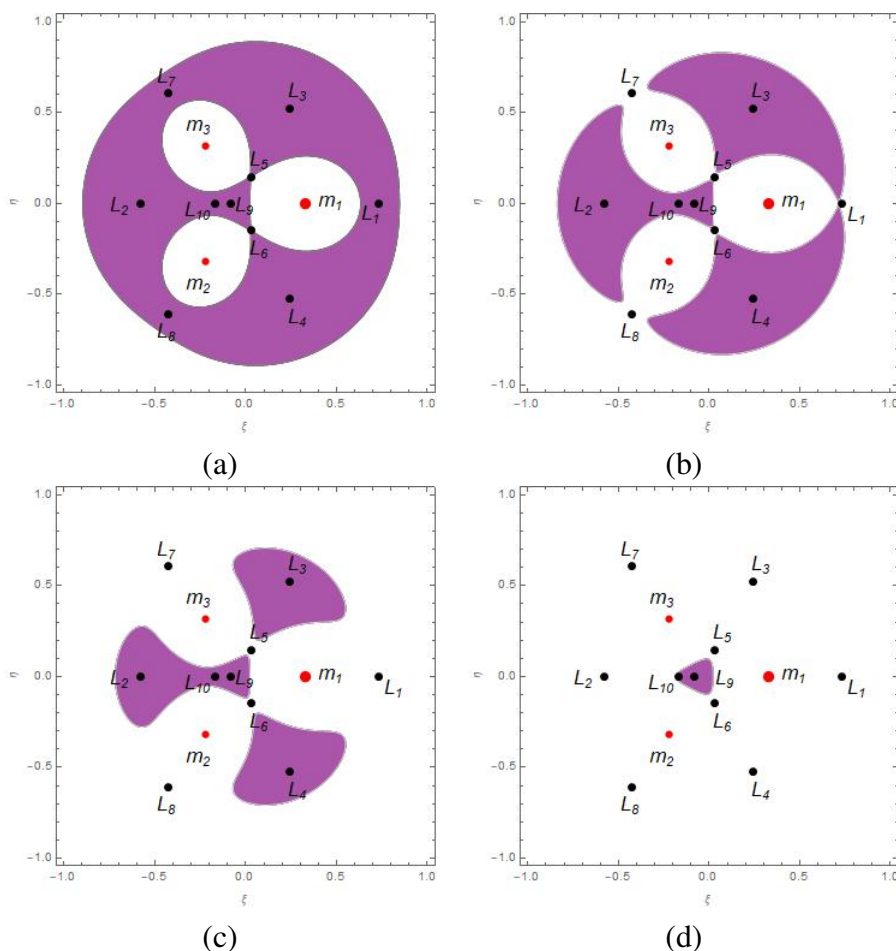


Figure 3. The ZVCs of the R4BP with variable mass for fixed values of the parameters $\gamma = 0.4$, $\mu = 0.3$ and the energy constant $C = C_{L_{5,6}} = 1.4245$ and varying α . a) $\alpha = 0.5$, b) $\alpha = 0.8$, c) $\alpha = 1.25$, d) $\alpha = 2.2$. Here the **black dots** represent the libration points and the **red dots** represent positions of the primaries. The white area corresponds to the region of motion and the purple area is the forbidden region

In Figure 4, panels (a)-(f), the ZVCs are drawn for fixed values of $\alpha = 1.5$, $\gamma = 0.4$, $C = C_{L_{5,6}} = 1.4048$ and for varying values of μ . In panel (a), $\mu = 0.005$, it is observed that the forbidden region contains the libration points $L_{1,2,5,6}$. The limiting situations exist at L_3 and L_4 where cusps are formed. The test particle is confined to move in the white circular region around the primary

m_1 but can not move in the shaded region. Also, it can move outside the shaded region. Thus, it can move from primary m_2 to m_3 and vice-versa but can't move to primary m_1 . In panel (b), $\mu = 0.01$, the horseshoe shaped forbidden region splits into two disjoint regions, one containing the libration point L_2 and other containing $L_{1,5,6}$. The corridors at L_3 and L_4 are available and the fourth body can now move from one primary to another primary and vice-versa but restricted to move in the shaded region. In panel (c), $\mu = 0.0137$, it is noticed that the forbidden regions constitute three branches in which two are tadpole shaped regions containing the libration points L_5 and L_6 respectively while the other island shaped region contains the libration point L_2 . A corridor is observed at L_1 where the test particle can move from one primary to another and vice-versa. In panels (d) and (e), it has been observed that the forbidden regions containing the libration points $L_{2,5,6}$ take the shapes of a flattened islands. In panel (f) $\mu = 0.3$, in this case there exist four collinear libration points and a sudden change in the pattern of forbidden region around L_2 is observed. A limiting situation is also observed at L_{10} where cusp is formed. Therefore, it is concluded that μ has substantial impact on the ZVCs.

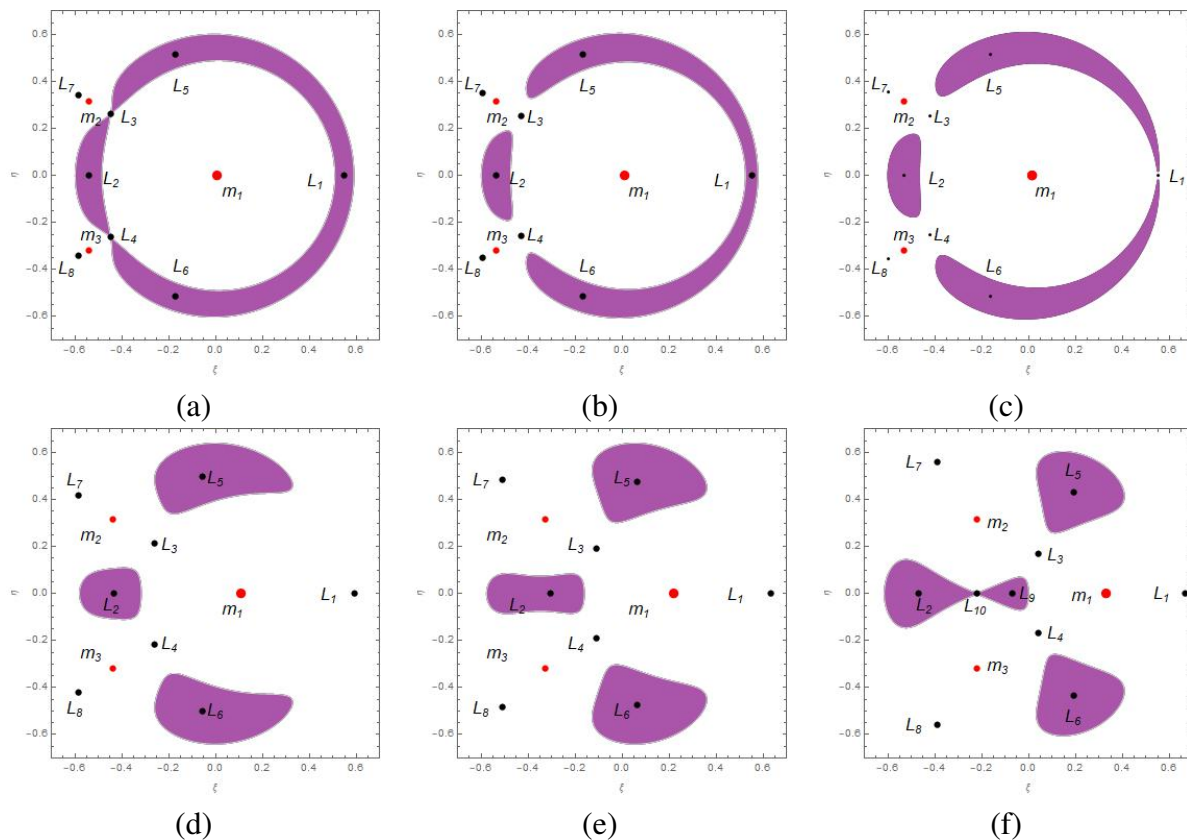


Figure 4. The ZVCs of the R4BP with variable mass for different values of μ and for fixed values of $\gamma = 0.4$, $\alpha = 1.5$ and the energy constant $C = C_{L_{3,4}} = 1.4048$. a) $\mu = 0.005$, b) $\mu = 0.01$, c) $\mu = 0.0137$, d) $\mu = 0.1$, e) $\mu = 0.2$ and f) $\mu = 0.3$. Here the **black dots** represent the libration points and the **red dots** represent the primaries. The white region is the region of motion and the purple region is the forbidden region

5. Stability of the libration points

If the test particle oscillates about a point when it is given a small displacement from it, the point is said to be stable point and if the test particle departs rapidly from the neighborhood of the point, the point is said to be unstable. The stability of the libration points has been examined in the restricted four body problem with variable mass. We denote the libration point by (ξ_0, η_0, ζ_0) (for a fixed time t) and to investigate its stability, we give a small displacement (u, v, w) from it, as:

$$\xi = \xi_0 + u, \quad \eta = \eta_0 + v, \quad \zeta = \zeta_0 + w, \quad (u, v, w \ll 1). \quad (13)$$

Using equations (13) in equations (9), the following variational equations are obtained

$$\begin{aligned} \ddot{u} - 2\dot{v} &= (W_{\xi\xi})_0 u + (W_{\xi\eta})_0 v + (W_{\xi\zeta})_0 w, \\ \ddot{v} + 2\dot{u} &= (W_{\eta\xi})_0 u + (W_{\eta\eta})_0 v + (W_{\eta\zeta})_0 w, \\ \ddot{w} &= (W_{\zeta\xi})_0 u + (W_{\zeta\eta})_0 v + (W_{\zeta\zeta})_0 w, \end{aligned} \quad (14)$$

where the subscript '0' in equations (14) indicates that the values are to be calculated at the respective libration point (ξ_0, η_0, ζ_0) and,

$$\begin{aligned} W_{\xi\xi} &= \left(1 + \frac{\alpha^2}{4}\right) + 3\gamma^{\frac{3}{2}} \left\{ (1-2\mu) \frac{(\xi - \sqrt{3}\mu\gamma^{1/2})^2}{\rho_1^5} + \mu \frac{(\xi + \frac{\sqrt{3}}{2}(1-2\mu)\gamma^{1/2})^2}{\rho_2^5} \right. \\ &\quad \left. + \mu \frac{(\xi + \frac{\sqrt{3}}{2}(1-2\mu)\gamma^{1/2})^2}{\rho_3^5} \right\} - \gamma^{3/2} \left(\frac{1-2\mu}{\rho_1^3} + \frac{\mu}{\rho_2^3} + \frac{\mu}{\rho_3^3} \right), \\ W_{\eta\xi} &= 3\gamma^{\frac{3}{2}} \left\{ (1-2\mu) \frac{(\xi - \sqrt{3}\mu\gamma^{1/2})\eta}{\rho_1^5} + \mu \frac{(\xi + \frac{\sqrt{3}}{2}(1-2\mu)\gamma^{1/2})(\eta + \frac{\gamma^{1/2}}{2})}{\rho_2^5} \right. \\ &\quad \left. + \mu \frac{(\xi + \frac{\sqrt{3}}{2}(1-2\mu)\gamma^{1/2})(\eta - \frac{\gamma^{1/2}}{2})}{\rho_3^5} \right\}, \\ &= W_{\xi\eta}, \\ W_{\eta\eta} &= 1 + \frac{\alpha^2}{4} + 3\gamma^{\frac{3}{2}} \left\{ (1-2\mu) \frac{\eta^2}{\rho_1^5} + \mu \frac{(\eta + \frac{\gamma^{1/2}}{2})^2}{\rho_2^5} + \mu \frac{(\eta - \frac{\gamma^{1/2}}{2})^2}{\rho_3^5} \right\} - \gamma^{3/2} \left(\frac{1-2\mu}{\rho_1^3} + \frac{\mu}{\rho_2^3} + \frac{\mu}{\rho_3^3} \right), \\ W_{\zeta\xi} &= W_{\xi\zeta} = 3\gamma^{\frac{3}{2}} \zeta \left\{ (1-2\mu) \frac{(\xi - \sqrt{3}\mu\gamma^{1/2})}{\rho_1^5} + \mu \frac{(\xi + \frac{\sqrt{3}}{2}(1-2\mu)\gamma^{1/2})}{\rho_2^5} + \mu \frac{(\xi + \frac{\sqrt{3}}{2}(1-2\mu)\gamma^{1/2})}{\rho_3^5} \right\}, \\ W_{\eta\zeta} &= W_{\zeta\eta} = 3\gamma^{\frac{3}{2}} \zeta \left\{ (1-2\mu) \frac{\eta}{\rho_1^5} + \mu \frac{(\eta + \frac{\gamma^{1/2}}{2})}{\rho_2^5} + \mu \frac{(\eta - \frac{\gamma^{1/2}}{2})}{\rho_3^5} \right\}, \\ W_{\zeta\zeta} &= 3\gamma^{\frac{3}{2}} \zeta^2 \left(\frac{1-2\mu}{\rho_1^5} + \frac{\mu}{\rho_2^5} + \frac{\mu}{\rho_3^5} \right) - \gamma^{3/2} \left(\frac{1-2\mu}{\rho_1^3} + \frac{\mu}{\rho_2^3} + \frac{\mu}{\rho_3^3} \right) + \frac{\alpha^2}{4}. \end{aligned}$$

For $\alpha \neq 0$, the coordinates of three primaries and their distances to the libration point (ξ_0, η_0, ζ_0)

change with time. Rewriting the Equations (14) in phase space as follows:

$$\begin{aligned} \dot{u} &= u_1, & \dot{v} &= v_1, & \dot{w} &= w_1, \\ \dot{u}_1 - 2v_1 &= (W_{\xi\xi})_0 u + (W_{\xi\eta})_0 v + (W_{\xi\zeta})_0 w, \\ \dot{v}_1 + 2u_1 &= (W_{\eta\xi})_0 u + (W_{\eta\eta})_0 v + (W_{\eta\zeta})_0 w, \\ \dot{w}_1 &= (W_{\zeta\xi})_0 u + (W_{\zeta\eta})_0 v + (W_{\zeta\zeta})_0 w. \end{aligned} \quad (15)$$

Using space-time inverse transformations $x = \gamma^{-1/2}\xi$, $y = \gamma^{-1/2}\eta$ and $z = \gamma^{-1/2}\zeta$, and taking

$$\begin{aligned} x' &= \gamma^{-1/2}u, & u' &= \gamma^{-1/2}u_1, \\ y' &= \gamma^{-1/2}v, & v' &= \gamma^{-1/2}v_1, \\ z' &= \gamma^{-1/2}w, & w' &= \gamma^{-1/2}w_1, \end{aligned}$$

the system (15) can be written as:

$$\begin{pmatrix} \frac{dx'}{dt} \\ \frac{dy'}{dt} \\ \frac{dz'}{dt} \\ \frac{du'}{dt} \\ \frac{dv'}{dt} \\ \frac{dw'}{dt} \end{pmatrix} = \begin{pmatrix} \frac{\alpha}{2} & 0 & 0 & 1 & 0 & 0 \\ 0 & \frac{\alpha}{2} & 0 & 0 & 1 & 0 \\ 0 & 0 & \frac{\alpha}{2} & 0 & 0 & 1 \\ (W_{\xi\xi})_0 & (W_{\xi\eta})_0 & (W_{\xi\zeta})_0 & \frac{\alpha}{2} & 2 & 0 \\ (W_{\eta\xi})_0 & (W_{\eta\eta})_0 & (W_{\eta\zeta})_0 & -2 & \frac{\alpha}{2} & 0 \\ (W_{\zeta\xi})_0 & (W_{\zeta\eta})_0 & (W_{\zeta\zeta})_0 & 0 & 0 & \frac{\alpha}{2} \end{pmatrix} \begin{pmatrix} x' \\ y' \\ z' \\ u' \\ v' \\ w' \end{pmatrix}. \quad (16)$$

The characteristic equation of the coefficient matrix given in equation (16) is:

$$\begin{aligned} \lambda^6 - 3\alpha\lambda^5 + \left(\frac{15}{4}\alpha^2 + P\right)\lambda^4 - \left(\frac{5}{2}\alpha^3 + P\alpha\right)\lambda^3 + \left(\frac{15}{16}\alpha^4 + \frac{3}{2}P\alpha^2 + Q\right)\lambda^2 \\ - \left(\frac{3}{16}\alpha^5 + \frac{1}{2}P\alpha^3 + Q\alpha\right)\lambda + \left(\frac{1}{64}\alpha^6 + \frac{1}{16}P\alpha^4 + \frac{1}{4}Q\alpha^2 + R\right) = 0, \end{aligned} \quad (17)$$

where

$$\begin{aligned} P &= 4 - (W_{\xi\xi})_0 - (W_{\eta\eta})_0 - (W_{\zeta\zeta})_0, \\ Q &= (W_{\xi\xi})_0(W_{\zeta\zeta})_0 + (W_{\eta\eta})_0(W_{\zeta\zeta})_0 + (W_{\xi\xi})_0(W_{\eta\eta})_0 - 4(W_{\zeta\zeta})_0 - [(W_{\xi\eta})_0]^2, \\ R &= -(W_{\xi\xi})_0(W_{\eta\eta})_0(W_{\zeta\zeta})_0 + (W_{\zeta\zeta})_0[(W_{\xi\eta})_0]^2, \end{aligned}$$

the values of $(W_{\xi\xi})_0$, $(W_{\eta\eta})_0$, $(W_{\zeta\zeta})_0$ and $(W_{\xi\eta})_0$ are same as in equations (14).

The eigenvalues of the equation (17) have been calculated numerically at various libration points for $\gamma = 0.4$, $0 < \mu \leq 1/3$, $0 \leq \alpha \leq 2.2$. We obtain at least one positive real root at each libration point under consideration. Therefore, we conclude that all the libration points are unstable.

6. Newton-Raphson basins of convergence

The Newton-Raphson basins of convergence, associated with the libration points, reflect various important properties of the dynamical system. Recently, many researchers have studied the Newton-Raphson basins of convergence in various dynamical system including different perturbing terms in the effective potential (for example, Baltagiannis and Papadakis (2011), Suraj et al. (2017), Suraj et al. (2017), Zotos (2016a), Zotos (2016b), Zotos (2017)). In order to study the

basins of convergence associated with the libration points, we apply the multivariate version of the Newton-Raphson iterative scheme. We scan the set of initial conditions to reveal that to which attractor these initial conditions converge. To solve the systems of multivariate function $f(\mathbf{X}) = 0$, we apply the iterative scheme

$$\mathbf{X}_{i+1} = \mathbf{X}_i - J^{-1}f(\mathbf{X}_i),$$

where J is the Jacobian matrix of $f(\mathbf{X}_n)$.

In the present problem, the system of differential equations are given by

$$W_\xi = 0,$$

$$W_\eta = 0.$$

With simple calculations, we get the iterative formula for each coordinate as:

$$\xi_{n+1} = \xi_n - \left(\frac{W_{\xi_n} W_{\eta_n \eta_n} - W_{\eta_n} W_{\xi_n \eta_n}}{W_{\xi_n \xi_n} W_{\eta_n \eta_n} - W_{\xi_n \eta_n} W_{\eta_n \xi_n}} \right), \quad \eta_{n+1} = \eta_n + \left(\frac{W_{\xi_n} W_{\eta_n \xi_n} - W_{\eta_n} W_{\xi_n \xi_n}}{W_{\xi_n \xi_n} W_{\eta_n \eta_n} - W_{\xi_n \eta_n} W_{\eta_n \xi_n}} \right),$$

where ξ_n, η_n denote the iterates at the n -th step of the Newton-Raphson iterative process. The subscripts denote the corresponding partial derivatives of the first and second order of $W(\xi, \eta)$. The algorithm of the Newton-Raphson method is as follows:- The algorithm initiates with an initial condition ξ_0, η_0 on the configuration plane and the process continues until one of the attractors (or libration points) is reached with some predefined accuracy. The initial conditions may or may not lead us to the attractors. The Newton-Raphson basins of attraction consists of all the initial conditions which converge to the specific attractor. To reveal the structures of the basins of attraction on the configuration plane (x, y) , we define a uniform grid which consists of 1024×1024 initial conditions, which are also called nodes and will be used as initial values of the numerical algorithm. The iterative procedure terminates only when an accuracy of 10^{-15} regarding the procedure of the libration points is reached. In our study, we have set the maximum number of iterations equal to 500.

It has been shown, how the geometry of the Newton-Raphson basins of attraction change with the change in the mass parameter μ and constant of proportionality α . We classify the initial conditions on $\xi\eta$ -plane and modern colour coded diagrams have been used to do the same. In all the diagrams, each pixel is assigned a particular colour according to the particular attractor (libration point). The minimum and maximum values of ξ and η are chosen different in each case to view the complete picture of the basins of attraction generated by the attractors.

6.1. Case I: when α varies

We study the effect of α in the interval $[0, 2.2]$. In Figure 5, we have shown a collection of colour coded graphs illustrating the Newton-Raphson basins of convergence for various values of α . The choice of initial conditions ξ_0 and η_0 is highly sensitive as even a slight change in the initial conditions leads to a completely different destination. Therefore, it is difficult to find which of the libration point, each initial condition is attracted by. We have observed that a change in α does not

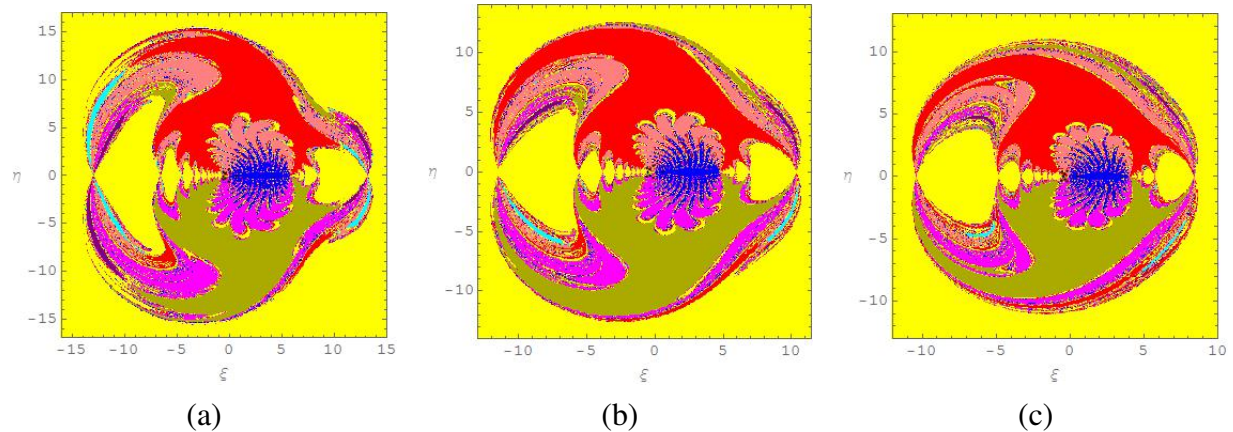


Figure 5. The Newton-Raphson basins of attraction on the configuration plane (ξ, η) when $\gamma = 0.4$ and $\mu = 0.019$. (a) $\alpha = 0.5$, (b) $\alpha = 1.5$, (c) $\alpha = 2.2$. The colour code denoting the attractors is as follows: L_1 (blue), L_2 (Yellow), L_3 (Red), L_4 (Darker Yellow), L_5 (Pink), L_6 (Magenta), L_7 (Cyan), L_8 (Purple)

follow a specific pattern. In Figure 5, panels (a)-(c), we have observed that these basins are symmetric about ξ -axis. An interesting phenomenon related to the extent of the basins of convergence is observed. The extent of basins of convergence corresponding to the non-collinear libration points is always finite, whereas the extent of attracting domains of the collinear libration point L_2 (yellow colour) extends to infinity. With the increase in α , the extent of basins of convergence corresponding to the non-collinear libration points, shrinks whereas corresponding to the collinear libration point L_2 , the extent of basins of convergence expands. For the libration point L_1 , the Newton-Raphson basins of attraction look like an exotic bug in blue colour with many legs and antennas whereas for the libration points L_5 and L_6 , constitute multiple wings of a butterfly. Some heart shaped curves originate at L_1 and increase continuously to the right of L_1 . We also notice that some tadpole shaped curves originate at the libration point L_2 and they increase to the left of L_2 continuously. The boundary of the basins of attraction are chaotic mixtures of the initial conditions corresponding to the libration points. It can be inferred that the maximum number of initial conditions on the configuration plane are attracted by the libration point L_2 .

In Figure 6, panels (a)-(c), the extent of basins of convergence corresponding to the non-collinear libration points is always finite, whereas the extent of attracting domains of the collinear libration point L_9 extends to infinity. As we increase the value of α , drastical changes are observed in the basins of attraction. Further, it is noticed from frame (c) that almost very few initial conditions are attracted by the libration points L_2 and L_{10} . In this case, the convergence of initial condition are extremely slow and it takes more than 500 iterations to converge to one of the libration point L_i ($i = 1, 2, \dots, 10$).

6.2. Case II: when μ varies

In Figure 7, panels (a)-(c) our aim is to study the effect of μ on the topology of Newton-Raphson basins of attraction. The extent of basins of convergence corresponding to the non-collinear libration points is always finite, whereas the extent of attracting domains of the collinear libration

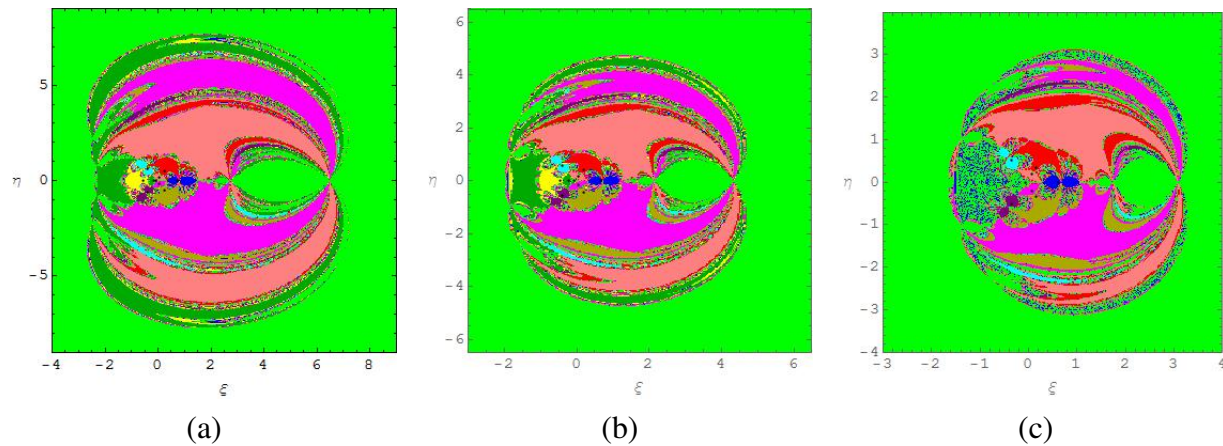


Figure 6. The Newton-Raphson basins of attraction on the configuration plane (ξ, η) when $\gamma = 0.4$ and $\mu = 0.3$ and α varies. (a) $\alpha = 0.5$, (b) $\alpha = 1.5$, (c) $\alpha = 2.2$. The colour code denoting the attractors is as follows: L_1 (blue), L_2 (Yellow), L_3 (Red), L_4 (Darker Yellow), L_5 (Pink), L_6 (Magenta), L_7 (Cyan), L_8 (Purple), L_9 (Green), L_{10} (Darker Green)

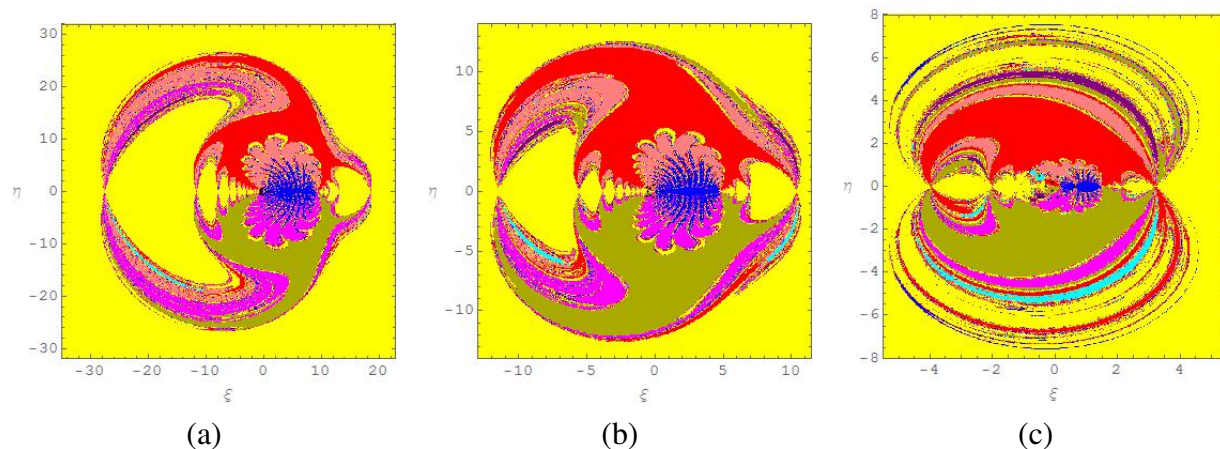


Figure 7. The Newton-Raphson basins of attraction on the configuration plane (ξ, η) when $\alpha = 1.5$, $\gamma = 0.4$ (a) $\mu = 0.005$, (b) $\mu = 0.019$, (c) $\mu = 0.2$. The color code denoting the attractors is same as in Figure 5

point L_2 extends to infinity. In this case, we have observed that there is no uniform pattern for the basins of attraction. We have noticed that the basins of convergence corresponding to finite domain shrink. The tadpole shaped regions near the primary m_1 decreases as we increase μ .

7. Discussion and conclusion

The main aim of this paper is to study the effect of the mass parameter (μ) and proportionality constant (α) on the existence, location and stability of the libration points in the R4BP with variable mass when the primaries are always in the Lagrange equilateral triangle configuration. It has been observed that there exist ten libration points out of which four are collinear and six are non-collinear for the case $\mu = 0.3$, $0 \leq \alpha \leq 1.5$, but the number of collinear libration points decrease from four to two for $\alpha = 2.2$ and number of non-collinear libration points remains same (refer

table 2). Whereas for $\mu = 0.019$ the number of libration points are always eight (two collinear and six non-collinear) for all $\alpha \in [0, 2.2]$ (Mittal et al. (2016)). The regions of motion for the parameters used are drawn and their effect are shown on regions of motion. We have further studied the stability of the libration points and found that all the libration points are unstable for all the values of the parameters used. The study ends with the section where the multivariate version of Newton-Raphson iterative scheme is applied to discuss the basins of convergence. Further, our analysis reveals that the parameters α and μ have significant impact on the geometry as well as on the topology of the attracting domain corresponding to each libration point.

In future, it is interesting to apply other type of iterative schemes and discuss the similarities as well as differences in the topology of the attracting domains corresponding to the libration points.

Acknowledgements

We are thankful to Centre of Fundamental Research in Space Dynamics and Celestial Mechanics (CFRSC), Delhi, India for providing necessary facilities required for this research work.

REFERENCES

- Abouelmagd, E.I. (2012). Existence and stability of triangular points in the restricted three-body problem with numerical applications, *Astrophys. Space Sci.*, Vol. 342, pp. 45–53.
- Aggarwal, R., Kaur, B. (2014). Robe's restricted problem of 2 + 2 bodies with one of the primaries an oblate body, *Astrophys. Space Sci.*, Vol. 352, No. 2, pp. 467–479.
- Asique, M.C., Umakant, P., Hassan, M.R. and Suraj, M.S. (2015a). On the photogravitational R4BP when third primary is an oblate/prolate spheroid, *Astrophys. Space Sci.*, Vol. 360, No. 13. doi:10.1007/s10509-015-2522-1.
- Asique, M.C., Umakant, P., Hassan, M.R. and Suraj, M.S. (2015b). On the R4BP when third primary is an oblate spheroid, *Astrophys. Space Sci.*, Vol. 357, No. 82. doi:10.1007/s10509-015-2235-5.
- Asique, M.C., Umakant, P., Hassan, M.R. and Suraj, M.S. (2016). On the photogravitational R4BP when the third primary is a triaxial rigid body, *Astrophys. Space Sci.*, Vol. 361, No. 379. doi:10.1007/s10509-016-2959-x.
- Asique, M.C., Umakant, P., Hassan, M.R., Suraj, M.S. (2017). On the R4BP when Third Primary is an Ellipsoid, *J. Astronaut Sci.*, Vol. 64, , No. 3, pp. 231–250.
- Baltagiannis, A.N. and Papadakis, K.E. (2011). Equilibrium points and their stability in the restricted four-body problem., *Int. J. Bifurc. Chaos Appl. Sci.*, Vol. 21, No. 8, pp. 2179–2193.
- Bhatnagar, K.B. and Hallan, P.P. (1978). Effect of perturbations in Coriolis and centrifugal forces on the stability of libration points in the restricted problem, *Celest. Mech.*, Vol. 18, pp. 105–112.

- Bhatnagar, K.B. and Chawla, J.M. (1979). A study of the Lagrangian points in the photogravitational restricted three-body problem, *Indian J. Pure Appl. Math.*, Vol. 10, No. 11, pp. 1443–1451.
- Euler, L. (1767). *De moto rectilineo trium corporum se mutuo attrahentium*, *Novo Comm. Acad. Sci. Imp. Petrop.*, Vol. 11, pp. 144–151.
- Kaur, B. and Aggarwal, R. (2012). Robe's problem: its extension to 2+2 bodies, *Astrophys. Space Sci.*, Vol. 339, No. 2, pp. 283–294.
- Kaur, B. and Aggarwal, R. (2013). Robe's restricted problem of 2+2 bodies when the bigger primary is a roche ellipsoid, *Acta Astronautica*, Vol. 89, pp. 31–37.
- Kaur, B. and Aggarwal, R. (2014). Robe's restricted problem of 2+2 bodies when the bigger primary is a roche ellipsoid and the smaller primary is an oblate body, *Astrophys. Space Sci.*, Vol. 349, No. 1, pp. 57–69.
- Kumar, V. and Choudhry, R.K. (1986). Existence of libration points in the generalised photogravitational restricted problem of three bodies, *Celest. Mech.*, Vol. 39, pp. 159–171.
- Kumari, R. and Kushvah, B.S. (2014). Stability regions of equilibrium points in restricted four-body problem with oblateness effects, *Astrophys. Space Sci.*, Vol. 349, No. 2, pp. 693–704.
- Meshcherskii, I.V. (1949). *Studies on the mechanics of bodies of variable mass*. GITTL, Moscow.
- Meshcherskii, I.V. (1952). *Works on the mechanics of bodies of variable mass*. GITTL, Moscow.
- Mittal, A., Ahmad, I. and Bhatnagar, K.B. (2009a). Periodic orbits generated by Lagrangian solutions of the restricted three body problem when one of the primaries is an oblate body, *Astrophys. Space Sci.*, Vol. 319, No. 1, pp. 63–73.
- Mittal, A., Ahmad, I. and Bhatnagar, K.B. (2009b). Periodic orbits in the photogravitational restricted problem with the smaller primary an oblate body, *Astrophys. Space Sci.*, Vol. 323, No. 1, pp. 65–73.
- Mittal, A., Aggarwal R., Suraj, M.S. and Bisht, V.S. (2016). Stability of libration points in the restricted four-body problem with variable mass, *Astrophys. Space Sci.* Vol. 361, No. 329, pp. 417–424. doi.org/10.1007/s10509-016-2901-2.
- Newton (1687). *Philosophiae Naturalis Principia Mathematica*, Royal Soc. Press, London.
- Papadouris, J.P. and Papadakis, K.E. (2013). Equilibrium points in the photogravitational restricted four-body problem, *Astrophys. Space Sci.*, Vol. 344, No. 1, pp. 21–38.
- Sharma, R.K. and Subba Rao, P.V. (1975). Collinear equilibria and their characteristic exponents in the restricted three-body problem when the primaries are oblate spheroids, *Celest. Mech.*, Vol. 12, pp. 189–201.
- Sharma, R.K. and Subba Rao, P.V. (1976). Stationary solutions and their characteristic exponents in the restricted three-body problem when the more massive primary is an oblate spheroid, *Celest. Mech.*, Vol. 13, pp. 137–149.
- Sharma, R.K. (1981). Periodic orbits of the second kind in the restricted three-body problem when the more massive primary is an oblate spheroid, *Astrophys. Space Sci.*, Vol. 76, No. 1, pp. 255–258.
- Shrivastava, A.K. and Ishwar, B. (1983). Equations of motion of the restricted problem of three bodies with variable mass, *Celest. Mech.*, Vol. 30, pp. 323–328.
- Singh, J. (2003). Photogravitational restricted three-body problem with variable mass, *Indian J. of Pure and Applied Math.*, Vol. 32, No. 2, pp. 335–341.

- Singh, J. and Ishwar, B. (1984). Effect of perturbations on the location of equilibrium points in the restricted problem of three bodies with variable mass, *Celest. Mech.*, Vol. 32, No. 4, pp. 297–305.
- Singh, J. and Ishwar, B. (1985). Effect of perturbations on the stability of triangular points in the restricted problem of three bodies with variable mass, *Celest. Mech.*, Vol. 35, pp. 201–207.
- Singh, J. and Leke (2010). Stability of photogravitational restricted three-body problem with variable mass, *Astrophys. Space Sci.*, Vol. 326, No. 2, pp. 305–314.
- Singh, J. and Vincent, A.E. (2015a). Effect of perturbations in the Coriolis and centrifugal forces on the stability of equilibrium points in the restricted four-body problem, *Few-Body Syst.*, Vol. 56, pp. 713–723.
- Singh, J. and Vincent, A.E. (2015b). Out-of-plane equilibrium points in the photogravitational restricted four-body problem, *Astrophys. Space Sci.*, Vol. 359, No. 38. doi: 10.1007/s10509-015-2487-0.
- Singh, J. and Vincent, A.E. (2016). Equilibrium points in the restricted four-body problem with radiation pressure, *Few-Body Sys.*, Vol. 57, pp. 83–91.
- Suraj, M.S., Aggarwal, R. and Arora, M. (2017). On the restricted four-body problem with the effect of small perturbations in the Coriolis and centrifugal forces, *Astrophys. Space Sci.*, Vol. 362, No. 159. doi:10.1007/s10509-017-3123-y.
- Suraj, M.S., Asique, M.C., Prasad, U., Hassan, M.R. and Shalini, K. (2017). Fractal basins of attraction in the restricted four-body problem when the primaries are triaxial rigid bodies, *Astrophys. Space Sci.*, Vol. 362, No. 211. doi:10.1007/s10509-017-3188-7.
- Suraj, M.S. and Hassan, M.R. (2014). Sitnikov restricted four-body problem with radiation pressure, *Astrophys. Space Sci.*, Vol. 349, No. 2, pp. 705–716.
- Suraj, M.S., Hassan, M.R. and Asique, M.C. (2014). The Photo-Gravitational R3BP when the Primaries are Heterogeneous Spheroid with Three Layers, *J. Astronaut. Sci.*, Vol. 61, No. 133. doi:10.1007/s40295-014-0026-9.
- Zotos, E.E. (2016a). Escape and collision dynamics in the planar equilateral restricted four-body problem, *Int. J. Non-Linear Mec.*, Vol. 86, pp. 66–82.
- Zotos, E.E. (2016b). Fractal basins of attraction in the plainar cicular restricted three-body problem with oblateness and radiation pressure, *Astrophys. Space Sci.*, Vol. 361, No. 181.
- Zotos, E.E. (2017). Revealing the basins of convergence in the planar equilateral restricted four-body problem, *Astrophys. Space Sci.*, Vol. 362, No. 2.